Quantifying the performance of automated GIS-based geomorphological approaches for riparian zones delineation using Digital Elevation Models

D. Fernández[1,2], J. Barquín[1], M. Álvarez-Cabria[1], and F. J. Peñas[1]

[1]: Environmental Hydraulics Institute "IH Cantabria", Universidad de Cantabria, PCTCAN. C/ Isabel Torres 15, 39011 Santander, Spain

[2] Present affiliation: Institute for Environmental Sciences, University Koblenz-Landau. Fortstrasse 7, 76829 Landau in der Pfalz, Germany

Correspondence to: D. Fernández (diegofgrm@gmail.com)

Abstract

Riparian zone delineation is a central issue for managing rivers and adjacent areas, however, criteria used to delineate them are still under debate. The area inundated by a 50-yr flood has been indicated as an optimal hydrological descriptor for riparian areas. This detailed hydrological information is usually only available for populated areas at risk of flooding. In this work we created several floodplain surfaces by means of two different GIS-based geomorphological approaches using Digital Elevation Models in an attempt to find hydrologically-meaningful potential riparian zones for entire river networks. Objective quantification of the performance of the two geomorphologic models is provided by analysing coinciding and exceeding areas with respect to the 50-yr flood surface in different river geomorphological types.

1 Introduction

Riparian areas are involved in different geomorphological, hydrological and ecological processes (Tabacchi et al., 1998; Naiman et al., 2005) and provide many services to society, such as reducing flood risk or improving the availability and quality of water (Staats and Holtzman, 2002; Hruby, 2009). Despite this, riparian zones are commonly under high pressure due to human activities and land-use transformation (for a review see Poff et al., 2011). The maintenance of riparian functions and values is of key importance and requires planning at catchment scale and to locate the optimal zones to conserve or restore riparian buffer strips. Additionally, the definition of riparian zone extent is an unavoidable issue when managing river corridors. There exist several different approaches to delineate riparian areas (e.g. McGlynn and Seiber, 2003; Dodov and Foufoula-Georgiou, 2006; Nardi et al., 2006), but the developing of a standard methodology for a geomorphologic tool for preliminary floodplain mapping is still an open research topic.

The delineation of riparian zones is highly dependant on what is understood as "riparian". Existing definitions are quite heterogeneous with respect to the zones encompassed by this term. While most authors use definitions matching with river banks and floodplains, others also include river channels (Naiman et al., 1993; USDA FS, 1994) or extend these zones to the slopes adjacent to floodplains (Ilhardt et al., 2000; Verry et al., 2004). By focusing on land adjacent to watercourses, there is agreement about the following riparian zone characteristics: (i) they are transitional zones between aquatic and terrestrial ecosystems (Gregory et al., 1991; NRC, 2002), (ii) their soil and vegetation characteristics are strongly influenced by free or unbound water in the soil that comes from elevated water tables and flooding by high waters (USDA NRCS, 1991; Naiman et al., 1993; USDA FS, 1994), (iii) they present gradients of environmental factors, ecological processes and biota (Gregory et al., 1991; NRC, 2002). Hence, the spatial and temporal distribution of vegetation in riparian areas is heavily influenced by flood regime (Gregory et al., 1991; Merrit et al., 2009; Naura et al., 2011) and responds to the array of hydrogeomorphic patches appearing along the fluvial network (Van Coller et al., 2000; Poole, 2002; Thorp et al., 2006). High flows (characterised by magnitude, duration and frequency) control the creation and destruction of landforms across the fluvial landscape, and limit the spread of non-riparian species (Merrit et al., 2009).

As an ecotone, riparian zone limits are fuzzy and defining discrete boundaries can be a difficult task. In addition, the extent of the riparian zone is not constant within the longitudinal dimension of rivers, as reflected in several studies on floodplain extent and associated parameters as a function of the contributing area (Bhowmik, 1984; Dodov and Foufoula-Georgiou, 2004). Despite of this, establishing fixed distances from water edge has been a common approach in riparian delineation for regulatory purposes (e.g. best management practices, Australian Rivers and Foreshores Improvement Act, Canadian Streamside Protection Regulation), with buffer widths ranging habitually from 10 to less than 50 m. In this regard, about 40 m is an averaged minimum buffer width necessary to maintain relevant riparian functions (Sutula et al., 2006, Clerici et al., 2011, 2013). However, fixed buffer approaches often result in oversized riparian areas in headwaters and confined valleys and undersized in lowlands and unconfined valleys (Holmes and Goebel, 2011). Some authors have dealt with this issue by establishing a buffer distance dependant on river order (e.g., Yang et al., 2007), although this approach is still not sensitive to local geomorphology as a river of a given order can show large valley morphology variability.

Recent approaches are setting aside fixed buffers and moving forward to more-objective criteria. Some of these criteria are based on physical attributes, such as soil characteristics (Palik et al., 2004) or hydrology (Hupp and Osterkamp, 1996; Osterkamp and Hupp, 2010). Others are based on biota, such as vegetation (Amundsen, 2003; Mac Nally et al., 2008) or amphibians (Perkins and Hunter, 2006). Most of these criteria demand information that is not usually available over large areas, or not with enough spatial resolution to delineate riparian areas. Geographical Information Systems (GIS) could be used to overcome this problem. Hence, several GIS-based methods have been published in the last decade regarding floodplain/riparian zone delineation. Most of them rely on a Digital Elevation Model (DEM) and water level data. A common approach consist in using water level data observed at gauging stations or simulated in a hydraulic model at several locations and extended them over the floodplain by interpolating water levels at each DEM cell (Noman et al., 2001). Other GIS-based methods are based on algorithms which calculate inundation depth (Dodov and Foufoula-Georgiu, 2006; Nardi et al., 2006) or riparian width (MCGlynn and Seibert, 2003) for each stream cell. These algorithms are obtained by performing regression between catchment area (obtained by terrain analysis from a DEM) and water level or riparian width data at several locations. All these methods delineate linear boundaries; instead, Clerici et al. (2011, 2013) have developed a GIS-based riparian zonation model which uses membership scores indicating the probability of belonging to the riparian zone based on natural vegetation presence and water influence. To sum up, a wide variety of DEM-based methods are available for preliminary floodplain/riparian zone extraction. The quantification of their performance is usually provided as a regression coefficient among catchment area and inundation depth or riparian width. However, this is not enough to provide complete clarification of the adjustment among modelled and real floodplain/riparian zone (e.g which of the two floodplain surfaces cover a larger area? Where along the river network are located the better and worst adjustments?)

The present study aims to: (i) delineate hydrologically-meaningful potential riparian zones for entire river networks using GIS-based geomorphologic approaches relying on DEMs and (ii) provide an objective quantification of the performance of the proposed geomorphologic models. To that end we created several geomorphologic floodplain surfaces using two different geomorphologic approaches and we evaluated their adjustment with respect to a hydrologic floodplain surface representing the real riparian zone. As the relationship between local geomorphology and floodprone area has been suggested to be river-type dependant (Rosgen, 1996) we performed the analyses distinguishing between river geomorphological types. We also compared the performance of two different methods to evaluate adjustment between the surfaces derived from geomorphological and hydrological criteria.

2 Study area

This study was developed in river catchments from the Cantabrian region, Northern Spain (Fig. 1). Cantabrian rivers have their source in the Cantabrian Cordillera, a mountain range which runs parallel to the Atlantic Ocean coast and reaches up to 2600m a.s.l. In the northern part of the region, rivers drain into the Atlantic Ocean. These rivers are short, with high slopes and high erosive power. The largest basins slightly exceed 1000 km^2 and 20 m^3s^{-1} of mean daily flow, with highly variable valley widths that rarely exceed 1.5 km in most of the middle and upper courses. This area has a humid oceanic temperate climate (Rivas-Martínez et al., 2004) with an average annual temperature of 14ºC and an average annual precipitation of 1200 mm. The southern part of Cantabria is dominated by a continental climate with an average annual temperature of 10ºC and an average annual precipitation of 700 mm. In this part of the region, rivers belong to extensive and complex river systems which flow into the Mediterranean and the Atlantic, and they present more gentle relief and wider maximum valley widths than northern basins. In this area, rivers are generally long and with a gentle slope, draining into the Atlantic Ocean (Duero river basin) and into the Mediterranean Sea (Ebro river basin). The riparian vegetation is dominated by oceanic alder groves (*Alnus glutinosa*) in the Atlantic draining catchments from almost sea level up to 700m and by submediterranean alder groves (*Alnus glutinosa*) in the southern draining catchments (Lara et al., 2004). Willow groves formed by *Salix atrocinerea* (Northern Cantabrian cordillera) and *Salix cantabrica* (Southern Cantabrian cordillera) replace alder groves when they deteriorate, soils are not deep enough or there are large flow fluctuations. Higher in altitude, ashes (*Fraxinus excelsior*) or hazelnuts (*Corylus avellana*) (R1-C8) might dominate riparian forest, while in steep valleys beech, oak and mixed Atlantic forest predominate. Finally, when riparian forests are impaired by human activities, the riparian vegetation is usually dominated by *Rubus sp.*, *Rosa sp.*, *Crataegus monogyna, Prunus spinosa* or even pasture formations. For a more detailed description of the study area see (Barquín et al., 2012).

3 Methods

The methods used in the present work (Fig.2) were organized as follows. First we described how we obtained the hydrological (section 3.1) and geomorphological (section 3.2) floodplain surfaces. Then we introduced the framework used for evaluating the adjustment (section 3.3) and the two different adjustment methods (section 3.4). Finally, we explained how we accounted for the influence of DEM spatial resolution (section 3.5).

3.1 Hydrological floodplain surface

The 50-yr flood has been indicated as an appropriate hydrological descriptor for riparian zones as it usually coincides with the first terrace or other upward sloping surface (Ilhardt et al., 2000). Moving outward this topographic boundary necessarily increases water table depth and the probability of finding vegetation species related to riparian ecosystems may rapidly decrease. Therefore, 50-yr flood was selected in the present study as the surface representing potential riparian zone.

The area flooded by the 50-yr flood was available from a previous flood risk assessment study in the study area (IH Cantabria, 2008). In this study hydrological modelling with HEC MHS (US Army Corps of Engineers, 2000) was used to derive flow data. A high resolution DEM (5-m spatial resolution, 1-m vertical accuracy), long series of precipitation data (more than 30 years) and information about land-use and soil type (1:50 000 scale) were used as model inputs. For each river basin, flow was calculated at several points that were representative of homogeneous sub-basins. On the other hand, river hydraulics modelling was performed using HEC-RAS (US Army Corps of Engineers, 2005) and HEC-Geo RAS module, which allows use of a DEM to derive required cross-section data. This model required as input several parameters influencing flow behaviour: Manning's number (in this study the authors used 0.04 for the channel and 0.06 for floodplains, although variations were introduced where more detailed information was available), coefficients of expansion (0.3) and contraction (0.1) and boundary conditions (the water level at the river mouth cross-section was that of the highest equinoctial tide).

3.2 Geomorphological floodplain surfaces

We used two different GIS-based geomorphologic approaches to generate geomorphological floodplain surfaces. We referred to the first one as bankfull depth (BFD) approach. BFD is the vertical distance from the deepest part of a channel to the bankfull elevation (Fig. 3), being the bankfull discharge the flow that fills a stream channel to the elevation of the active floodplain (Wolman and Leopold, 1957). Hence, BFD approach consists in generating a surface which intersects valley walls at a given number of BFD above the channel. We referred to the second method as the path distance (PD) approach. PD is the least accumulative cost distance to the river channel when accounting for slope and elevation change, indicating the relative costs of moving from the stream cells up into the stream valley. The PD approach uses a raster showing the PD value for each cell to generate a surface covering all the locations along a river network which are encompassed by a certain path distance to the river channel. Both BFD and PD approaches require a DEM and a stream line as inputs to generate the floodplain surfaces. Additionally, BFD approach also requires BFD values in each segment of the river network. Before describing BFD and PD approaches, we described how we obtained the river network and BFD values.

3.2.1 River network and BFD values

The river network was derived using the analysis toolkit "NetMap" (http://www.netmaptools.org; Benda et al., 2007, 2009) following the procedure described by Benda et al. (2011). Hence, the network was delineated using flow directions inferred from a high-resolution DEM (5-m spatial resolution, 1-m vertical accuracy), using the algorithms described by Clarke et al. (2008). In flat areas, DEMs usually contain cells that are completely surrounded by other cells at the same or higher elevation. These cells act as sinks to overland flow when deriving a river network using flow direction (Martz and Garbrecht, 1998). To solve this problem, we enforced drainage in low relief areas (slope less than 30%) by lowering two meters the elevation of stream cells in the DEM using GIS data on channel real locations. Then the channel network was divided into channel segments (500–1000 m) and split at confluences, as they are supposed to produce changes in channel and floodplain morphologies (Benda et al., 2004). This resulted in river reach longitudes ranging from 3 to 850 m (Fig. 4a).

Bankfull depth (BFD) was estimated for each river segment using a regional regression of drainage area (*A*) and mean annual precipitation (*P*) to field measured depths over a range of channel sizes encompassing 195 river sites in the region of Cantabria (selected in areas with little to no engineered works). The results of this analysis yielded the following equation (Eq. 1):

$$BFD = 0.63 A^{0.1731} P^{0.1516} \qquad (1)$$

This model has been used in other recent applications (Benda et al. 2011) and it was the only one available at the time of pursuing this study for the Cantabrian region. However, it should be noted that BFD estimates might present deviations from observed values ($p < 0,001$; $R^2=0,12$), as BFD is highly sensible to local channel morphology (REF) and the present model only includes catchment area an mean annual precipitation.

3.2.2 BFD approach

The area bordering a stream that will be covered by water at a flood stage of twice the maximum BFD is called the floodprone area and corresponds on average to that which gets flooded by the 50-yr flood (Rosgen, 1996). However, floodprone height ranges from 1.3 times the BFD in rivers of Rosgen's type E (low-gradient meandering rivers) to 2.7 times the BFD in rivers of type A (highly-entrenched streams), and generally includes the active floodplain and the low terrace (Rosgen, 1996). Based on Rosgen’s empirical data, valley width at a height of approximately 2 times the BFD must coincide with the surface flooded by 50-yr flood. However, this relationship may be different when modelling in a GIS environment. Hence, we derived several geomorphologic floodplain surfaces using different bankfull depth heights ranging from 0.25 to 3 using steps of 0.25 (Fig. 4b).

To that end we used NetMap tools to transform the DEM (we used a 10-m DEM instead of the 5-m DEM due to computational limitations) into a raster where each cell was associated with the closest river segment (in Euclidean distance) presenting the fewest and smallest intervening high points. Cell values showed then the elevation difference (in terms of BFD) among the cell and its associated channel. Using this raster, it was possible to assess valley width at an elevation equivalent to a given number of BFDs for each river segment, and therefore generate geomorphological floodplain surfaces (polygon shapefile format) using the range of BFDs cited above. Hereafter we will refer to these surfaces as BFD-*X*, being *X* the factor multiplying bankfull depth (e.g. BFD-1.25).

3.2.3 <u>PD approach</u>

A PD raster was derived using the PD tool in ArcGis software (ESRI, 2011). PD tool required the following inputs: the river network (polyline shapefile) to identify stream cells, a DEM (a 10-m DEM, in order to be comparable with the surfaces generated by the BFD approach) as a surface raster and a slope raster as a cost layer. Then we used the reclassify tool to derive several surfaces (polygon shapefiles) corresponding with path distance threshold values ranging from 50 to 350 m using steps of 50 m (Fig. 4c). This range was determined by querying the values of several cells in the PD raster located at the edge of the 50-yr flood in different valley morphologies. Hereafter we will refer to the generated surfaces as PD-*Y*, being *Y* the threshold value used to generate that surface (e.g. PD-250).

3.3 Framework for evaluating the adjustment

Previous to analyse the adjustment between geomorphologic floodplain surfaces and the hydrologic floodplain surface, we developed a framework for this analysis. First, we create a geomorphological typology for the river network in order to take into account valley morphology when evaluating the adjustment, as it is valley dependant (Rosgen, 1996; see section 3.2.2). Second, we discarded those river segments where 50-yr flood was not available or presenting significant flood restrictions.

3.3.1 River types

The geomorphological attributes used to define river types were: channel and riverbank slope (considering as riverbank zone a buffer of 200m from the river channel), valley floor width and riverbank geological hardness. These four attributes are related with the flood height at a given location. Thus, channel slope is important to distinguish among high-energy straight rivers and low-energy meandering rivers. Both riverbank slope and valley floor width characterise cross-section topography for each river reach. And last, riverbank geological hardness differentiates those locations where river flows across alluvial easily-erodible material from those flowing across hard difficult-erodible geological substrate. Valley floor width is difficult to define for some valley morphologies, especially in V-shaped valleys. Generally, the edge of the valley floor is located in the first terrace or other major sloping surface, which usually corresponds with the 50-yr flood (Ilhardt et al., 2000). At the same time and as cited above, 50-yr flood corresponds on average to a flood stage of twice the maximum BFD (Rosgen, 1996). Hence, we used valley width at a height of two times the BFD as an approximation of the real valley width.

Channel slope and riverbank slope were calculated at the endpoint of each segment from the DEM. Valley floor width was obtained from BFD-2 surface, derived as described in section 3.2.2. Riverbank geological hardness was derived from the Spanish lithostratigraphic map (source: Geological and Mining Institute of Spain; spatial scale: 1:200 000). To that end we reclassified original geological classes into broader ones and then we assigned them a numerical value based on geological hardness (see Snelder et al., 2008 for details). This map was then converted into a raster layer. Finally we obtained riverbank hardness for each river reach using NetMap tools.

The four geomorphological attributes were finally used to classify the river network in geomorphological types by using PAM (partition around medoids) clustering in R software (R Development Core Team, 2008), previous data standardization. PAM clustering was performed using different pre-established numbers of clusters (3, 4 and 5). Then, we analysed the characteristics of each cluster (geomorphological type) with respect to the four geomorphological attributes using boxplots.

3.3.2 River network pruning

The 50-yr flood was not available for headwaters (Strahler order 1 and 2). From the 427 km where this information was available, we discarded those river segments presenting significant flood restrictions. We considered as significant restrictions all bank reinforcements or embankments longer than 100 m. We also excluded river reaches located downstream dams. The remaining river network comprised 321 km of rivers.

3.4 Adjustment methods

First, each geomorphological surface was divided based on river types using ArcGis software (ESRI, 2011), and the total area in each type was calculated. Then we evaluated the adjustment of each surface with respect to the 50-yr flood using two different methods:

(i) Minimum exceeding score (Eq. 2). This method combines the two possible exceeding surfaces: geomorphological surface exceeding area (GSEA) and 50-yr flood exceeding area (T50EA; Fig. 5). GSEA is the area of the geomorphological surface exceeding the 50-yr flood, while the T50EA is the area of the 50-yr flood not covered by the geomorphological surface. This latter parameter results from subtracting the coinciding area (CA; Fig. 5) from the 50-yr flood. The optimal geomorphological surface is that achieving the lowest minimum exceeding score.

$$\text{Minimum exceeding score} = \text{T50EA} + \text{GSEA} \quad (2)$$

(ii) Total area (Eq. 3). This method does not look at coinciding or exceeding areas, but only considers the deviance between the value of the area occupied by the geomorphological surface and the value of the area covered by the 50-yr flood. Total area optimum value is 100, and values above or below are considered as deviations. This condition may not reflect an "optimum adjustment", but as all geomorphological surfaces and the 50-yr flood are supposed to be sensitive to geomorphology, we considered exploring this possibility.

$$\text{Total area} = \frac{\text{geomorphological surface total area}}{\text{area covered by the 50 - yr flood}} \times 100 \quad (3)$$

3.5 Influence of DEM spatial resolution

As the DEM is the main input in our geomorphological approaches we wanted to test the influence of DEM spatial resolution in the performance of the present methodology. To that end, we have derived again all the geomorphologic floodplain surfaces under the BFD and PD approaches using a 30-m DEM, and compared their adjustment with the 50-yr flood as described in section 3.4.

4 Results

Cluster analysis showed that increasing the number of clusters (from 3 to 5) didn't produce an increase in classification strength (not shown). Hence, we chose three groups (clusters) to gain in simplicity and because the resulting groups highly reflect valley morphologies in our study area (see Fig. 1). The first of these groups included 1782 cases and corresponded with open valleys, as it presented the widest valleys (average >200 m), the lowest geological hardness and the lowest channel and stream bank slopes (average of 6 degrees and 13%, respectively; Fig. 6). The second one encompassed 1953 cases and corresponded with shallow-vee valleys presenting intermediate characteristics between the other two groups. Finally, the third group included 1908 cases and corresponded with deep-vee valleys and gorges, as it showed narrower valley widths (average <50 m), high geological hardness and the steepest channel and stream bank slopes (average of 22 degrees and 50%, respectively).

All geomorphological floodplain surfaces (despite of DEM spatial resolution) were sensitive to valley morphology, being narrower in constrained valleys due to closer and steeper slopes. By incrementing the factor multiplying BFD or the PD threshold value, geomorphological surfaces became wider and filled those gaps that lower threshold values can not fill (corresponding with low hills located in the valley bottom). The PD approach produced wider surfaces than BFD in unconstrained valleys, while the opposite trend was found in constrained valleys.

When using the 10-m DEM the adjustment between geomorphological and hydrological floodplain surfaces, in terms of coinciding and exceeding areas, showed the same general trend for all river types and the two geomorphological approaches (Fig. 7). As it was expected, increasing the geomorphological surface (by increasing the factor multiplying BFD or increasing the PD threshold value) increased CA, and therefore decreased T50EA. However, increasing the geomorphological surface also increased GSEA. Besides, the rate of increase of

GSEA was greater than that of CA, except in deep-vee valleys, where they presented almost the same rate. Intersection between T50EA and GSEA graphically indicates the optimal geomorphological surface. This intersection occurred at larger geomorphological surfaces when moving from open valleys to more entrenched ones, although there were no differences between open and shallow vee valleys. Despite the homogeneity in the above cited trends, the BFDAC reaches higher CA values than path distance. Consequently, PD reached higher T50EA values than BFD approach. However, both approaches showed similar values for GSEA. All these general trends cited above also occurred in open and shallow-vee valleys when using a 30-m DEM (Fig. 8). Coinciding and exceeding areas were also similar (except for PD approach when using low PD values), although the intersection of T50EA and GSEA occurred at lower threshold values (except for BFD approach in open valleys). Regarding deep-vee valleys, 30-m DEM produced almost the similar surface for all the range of thresholds used in both approaches (so CA, GSEA and T50EA follow a nearly horizontal line in Fig. 8). Besides, for PD approach GSEA was always higher than CA.

Total area method for evaluating the adjustment between the hydrological and geomorphological floodplain surfaces pointed out the same optimum threshold as the graphical intersection of GSEA and T50EA for both BFD and PD approaches (Fig. 9; only 10-m DEM adjustment is presented, as similar patterns are found for open and shallow vee valleys when working with a 30-m DEM). When using minimum exceeding score, only BFD complied with this statement. The total area method showed a positive linear relationship between the value defining the geomorphological surface and its total area. The slope of this relationship became steeper when moving from deep vee to open valleys. The BFD value that best matched the 50-yr flood was BFD-0.5 in open and shallow vee valleys an 1.25 in deep vee valleys. For PD approach, optimal adjustment occurred at PD-200 in open and shallow vee valleys and PD-350 in deep vee valleys. The adjustment of optimal geomorphological surfaces with respect to the 50-yr flood is shown in Fig. 10.

5 Discussion and conclusion

In this work we showed how automated GIS-based geomorphologic approaches can be used to obtain a 50-yr-flood-matching riparian zone. Both methods did not produce a complete adjustment among hydrological and geomorphological floodplain surfaces, however, the geomorphological derived surfaces present the following advantages: (i) sensitivity to topography, (ii) few inputs required and (iii) possibility of covering large areas. Hence, they constitute a remarkable improvement with respect to fixed buffer approaches and provide useful information for management in areas lacking hydrological data. They are, however, still not suitable for purposes requiring highly accurate data, such as flood damage prevention. Our methodology were strengthened by taking into account the influence of the following parameters: geomorphological approach, valley type, adjustment method and DEM spatial resolution. All of these parameters are discussed below.

Regarding geomorphological approach performance, both BFD and PD showed sensitivity to floodplain morphology and seemed valid to delineate riparian areas. BFD approach performance is better as the resulting geomorphological floodplain surfaces correspond with higher CA (10–19% depending on valley type) and lower GSEA (12–24 %) and T50EA (10–19 %) than those for PD when using a 10-m DEM. (larger differences among performance correspond with deep vee valleys). These differences among both approaches are reduced by two thirds when using a 30-m DEM, although BFD approach performed better than PD also at this resolution. On the other hand, PD approach does not require BFD values for each river reach in the network and it can be rapidly calculated in GIS. Moreover, the quality of the BFD regional model is important when there are not hydrological surfaces that could be used to match with the BFD estimated surfaces. In our model, BFD values were oversized, so we obtained optimal adjustment with the hydrological floodplain at lower values than those obtained by Rosgen (1996). To sum up, the choice of the proper geomorphological method depends on the resources and accuracy required. Besides, both BFD and PD approaches present the advantage of being suitable to account for the gradients present in riparian zones by assigning "membership to riparian zones" scores to each band defined by a different threshold value (the lesser is the threshold value, the higher must be the membership score as the river influence is also higher).

Despite of differing in characteristics as streamside slope or valley width, there is no need of distinguishing between open and shallow vee valleys (as defined in this study) when using our geomorphologic approaches to delineate riparian areas, as the same optimal geomorphological floodplain surface is obtained for both valley types. However, deep vee valley and gorges (constrained river reaches) require higher BFD values than unconstrained rivers to match with the 50-yr flood, as described also by Rosgen (1996). Hence, at least this two categories (constrained-unconstrained) should be taken into account. Beside, the less is the degree of constrainment, the worst is the adjustment in terms of GSEA. Similar results were obtained by Sutula et al. (2006). This may be due to the fact that unconstrained valleys present more complex fluvial landscapes than constrained ones. We have also considered that tributary confluences may also partly explain the disarrangement between geomorphological surfaces and the 50-yr flood, as they have not been considered in defining river types. In general terms they result in lower channel gradients and wider channel and floodplains (Benda et al., 2004; Fig. 11a). However, topographic constrains such as steep riverbank slopes or hardly-erodible riverbank materials seemed to be more determinant of floodplain width than confluence effects at some large channel confluences in our study area (e.g., Fig. 11b, where the main channel is the Deva River and Quiviesa and Bullón are large tributaries). Hence, it does not seem appropriate to include a variable accounting for confluence effects when classifying valley type, at least in mountainous study areas such as in here. In addition, we do find larger fluvial landscapes immediately above and below valley constrictions (Fig. 11c), as commented in Benda et al. (2001).

Minimum exceeding score and total area, the two methods used to determine the geomorphological floodplain surface that best matches the 50-yr flood, pointed out the same threshold value for BFD but not for PD approach. Despite the fact that total area is more subjective than minimum exceeding score, it seems to be more reliable as it always matches with the graphical intersection of T50EA and GSEA. Moreover, attention should be paid when using the minimum exceeding score in deep vee valleys. This method could suggest that any geomorphological surface is valid in these valleys, as the scores they produce with the different surfaces are all close to the optimum. By looking at total area it can be seen that this is not true, as moving backward or forward the optimum value significantly causes rapid deviation from 100% of total area, and this is reflected in exceeding and coinciding area combinations away from the optimum.

Results were dependant on DEM spatial resolution, as suggested in other studies dealing with riparian delineation (Nardi et al., 2006; Sutula et al., 2006; Abood and Maclean, 2011). In our study area, 10 and 30-m DEM resulted in similar adjustment in open and shallow vee valleys, regardless of the geomorphological approach used. 30-m DEM, however, proved to be an unsuitable input for delineating riparian zones in deep vee valleys as they occur in upper reaches, where rivers are narrow. Accordingly, the minimum DEM spatial resolution to be used depends on river and valley dimensions. Based on the differences between 10 and 30-m DEM performance, significant improvement is expected when using higher spatial resolutions (e.g. 5 m), especially when using PD-approach.

In conclusion, our results suggest that using GIS to delineate sensitive-to-geomorphology hydrologically-meaningful riparian zones is feasible and relatively easy and fast. However, this task does,require local calibration in order to find an optimal threshold value for the geomorphological approach which maximizes the coinciding and minimizes the exceeding with respect to the hydrological surface. Our results also suggest that this optimal threshold value depends on: valley morphology (constrained valleys require higher values unconstrained ones) and DEM spatial resolution.

Acknowledgements. We would like to thank to Lee Benda and Daniel Miller (Earth Systems Institute, CA, USA) for their collaboration and support at different stages of this research. We also thank Fernando Nardi and two anonymous referees for their valuable comments to the manuscript. Finally, We thank Ben P. Gouldby for the linguistic revision of the manuscript. This study was partly funded by the Spanish Ministry of Science and Innovation as part of the project MARCE (Ref: CTM-2009-07447) and by the Program of Postdoctoral Fellowships for Research Activities of the University of Cantabria (published by resolution on 17 January 2011).

REFERENCES

Abood, S. and Maclean, A.: Modeling riparian zones utilzing DEMs, flood height data, digital soil data and wetland inventory via GIS, in: American Society of Photogrammetry and RemoteSensing (ASPRS) 2011 Annual Conference, edited by: ASPRS, Milwaukee, Wisconsin, 1–5 May 2011, 2011.

Amundsen, K. J.: Mapping Riparian Vegetation in the Lower Colorado River Using Low Resolution Satellite Imagery, Cleveland State University, USA, 2003.

Barquín, J., Ondiviela, B., Recio, M., Álvarez-Cabria, M., Peñas, F. J., Fernández, D., Gómez, A., Álvarez C., and Juanes, J. A.: Assessing the conservation status of alder-ash alluvial forest and Atlantic salmon in the Natura 2000 river network of Cantabria, Northern Spain, in: River Conservation and Management: 20 years on, edited by: Boon, P. J. and Raven, d. P. J., Wiley-Blackwell, Chichester, West Sussex, UK, 2012.

Benda, L., Poff, N. L., Miller, D., Dunne, T., Reeves, G., Pess, G., and Pollock, M.: The network dynamics hypothesis: how channel networks structure riverine habitats, Bioscience, 54, 413–427, 2004.

Benda, L., Miller, D., Andras, K., Bigelow, P., Reeves, G., and Michael, D.: NetMap: a new tool in support of watershed science and resource management, Forest Sci., 53, 206–219, 2007.

Benda, L., Miller, D., Lanigan, S., and Reeves, G.: Future of applied watershed science at regional scales, Eos Transactions AGU, 90, p. 156, doi:10.1029/2009EO180005, 2009.

Benda, L., Miller, D., and Barquín, J.: Creating a catchment scale perspective for river restoration,Hydrol. Earth Syst. Sci., 15, 2995-3015, doi:10.5194/hess-15-2995-2011, 2011.

Bhowmik, N. G.: Hydraulic geometry of floodplains, J. Hydrol., 68, 369– 374, 1984.

Clarke, S. E., Burnett, K. M., and Miller, D. J.: Modeling streams and hydrogeomorphic attributes in Oregon from digital and field data, J. Am. Water Resour. As., 44, 459–477, 2008.

Clerici, N., Weissteiner, C. J., Paracchini, M. L., and Strobl, P.: Riparian zones: where green and blue networks meet. Pan-European zonation modelling based on remote sensing and GIS, Joint Research Centre of the European Comission, Luxembourg, Technical Report, 60 pp., 2011.

Clerici, N., Weissteiner, C. J., Paracchini, M. L., Boschetti, L., Baraldi, A., and Strobl, P.: Pan-European distribution modelling of stream riparian zones based on multi-source Earth Observation data, Ecol. Ind., 24, 211-223, 2013.

Dodov, B., and Foufoula-Georgiou, E.: Generalized hydraulic geometry: Derivation based on multiscaling formalism, Water Resour. Res., 40, W06302, doi:10.1029/2003WR002082, 2004.

Dodov, B. and E. Foufoula-Georgiou, E.: Floodplain Morphometry Extraction From a High-Resolution Digital Elevation Model: A Simple Algorithm for Regional Analysis Studies, IEEE Geosci. Remote Sens. Lett., 3, 2006.

Environmental Systems Research Institute (ESRI): ArcGIS Desktop: Release 10, Environmental Systems Research Institute, Redlands, CA, USA, 2011.

Gregory, S. V., Swanson, F. J., McKee, W. A., and Cummins, K. W.: An ecosystem perspective of riparian zones, Bioscience, 41, 540–551, 1991.

Hawes, E. and Smith, M.: Riparian Buffer Zones: Functions and Recommended Widths, Eightmile River Wild and Scenic Study Committee, 15, Yale School of Forestry and Environmental Studies, April 2005.

Holmes, K. L. and Goebel, P. C.: A functional approach to riparian area delineation using geospatial methods, J. Forest., 109, 233–241, 2011.

Hruby, T.: Developing rapid methods for analyzing upland riparian functions and values, Environ. Manage., 43, 1219–1243, 2009.

IH Cantabria: Desarrollo de la documentación técnica y cartográfica para la redacción del plan de protección civil ante el riesgo de inundaciones de la Comunidad Autónoma de Cantabria, Dirección General de Protección Civil, Consejería de Presidencia, Gobierno de Cantabria, Santander, Spain, Technical Report, 12 pp., 2008.

Hupp, C. R. and Osterkamp, W. R.: Riparian vegetation and fluvial geomorphic processes, Geomorphology, 14, 277–295, 1996.

Ilhardt, B. L., Verry, E. S., and Palik, P. J.: Defining riparian areas, in: Riparian Management in Forests of the Continental Eastern United States, edited by: Verry, E. S., Hornbeck, J. W., and Dollof, C. A., Lewis Publishers, Boca Raton, Florida, USA, 2000.

Lara, F., Garilleti, R., and Calleja, J. A.: La vegetación de ribera de la mitad norte Española, Monografias, 81, 536, 2004.

Mac Nally, R., Molyneux, G., Thomson, J. R., Lake, P. S., and Read, J.: Variation in widths of riparian-zone vegetation of higher-elevation streams and implications for conservation management, Plant Ecol., 198, 89–100, 2008.

Martz, L. W. and Garbrecht, J.: The treatment of flat areas and depressions in automated drainage analysis of raster digital elevation models, Hydrol. Process., 12, 843–855, 1998.

McGlynn, B. L., and Seibert, J.: Distributed assessment of contributing area and riparian buffering along stream networks, Water Resour. Res., 39, 1082, doi:10.1029/2002WR001521, 2003.

Merritt, D. M., Scott, M. L., Poff, N. L., Auble, G. T., and Lytle, D. A.: Theory, methods and tools for determining environmental flows for riparian vegetation: riparian vegetation-flow response guilds, Freshwater Biol., 55, 206–225, 2009.

Naiman, R. J., Décamps, H., and Pollock, M.: The role of riparian corridors in maintaining regional biodiversity, Ecol. Appl., 3, 209–212, 1993.

Naiman, R. J., Décamps, H., and McClain, M.: Riparia: Ecology, Conservation, and Management of Streamside Communities, Elsevier Academic Press, 430, San Diego, California, USA, 2005.

Nardi, F., Vivoni, E. R. and Grimaldi, S.: Investigating a floodplain scaling relation using a hydrogeomorphic delineation method, Water Resour. Res., 42, W09409, doi:10.1029/2005WR004155, 2006.

National Research Council (NRC), Committee on Riparian Zone Functioning and Strategies for Management: Riparian areas: functions and strategies for management, National Academy Press, Washington, DC, USA, 444, 2002.

Naura, M., Sear, D., Álvarez-Cabria, M., Peñas, F. J., Fernández, D., and Barquín, J.: Integrating monitoring, expert knowledge and habitat management within conservation organisations for the delivery of the water framework directive: a proposed approach, Limnetica, 30, 427–446, 2011.

Noman, N. S., Nelson, E. J. and Zundel, A. K.:Review of automated floodplain delineation from digital terrain models, J. Water Res. Pl., 127, 394–402, 2001.

Osterkamp, W. R. and Hupp, C. R.: Fluvial processes and vegetation – glimpses of the past, the present, and perhaps the future, Geomorphology, 116, 274–285, 2010.

Palik, B. J., Tang, S. M., and Chavez, Q.: Estimating riparian area extent and land use in the Midwest, Gen. Tech. Rep. NC-248., Department of Agriculture, Forest Service, North Central Research Station, St. Paul, MN, 28, 2004.

Perkins, D. W. and Hunter, M. L.: Use of amphibians to define riparian zones along headwater streams in Maine, Can. J. Forest. Res., 36, 2124–2130, 2006.

Poff, B., Koestner, K. A., Neary, D. G., and Henderson, V.: Threats to riparian ecosystems in Western North America: an analysis of existing literature, J. Am. Water Resour. As., 47, 1241–1254, 2011.

Poole, G. C.: Fluvial landscape ecology: addressing uniqueness within the river discontinuum, Freshwater Biol., 47, 641–660, 2002.

R Development Core Team: R: A language and environment for statistical computing, Vienna, Austria, software 3-900051-07-0, 2008.

Rivas-Martínez, S., Penas, A., and Díaz, T. E.: Bioclimatic Map of Europe, in: Bioclimates, León University, Cartographic Service, León, Spain, 2004.

Rosgen, D. L.: Applied river morphology, Wildland Hydrology, Pagosa Springs, CO, USA, 1996.

Snelder, T., Pella, H., Wasson, J.-G., and Lamouroux, N.: Definition procedures have little effect on performance of environmental classifications of streams and rivers, Environ. Manage., 42, 771–788, 2008.

Staats, J. and Holtzman, S.: Keeping water on the land longer – Healthy streams through bringing people together, University of California Water Resources Center, Stevenson, WA, USA, 2002.

Sutula, M., Stein, E. D., and Inlander, E.: Evaluation of a method to cost-effectively map riparian areas in Southern California coastal watersheds, Technical Report 480, Southern California Coastal Water Research Project (SCCWRP), 2006.

Tabacchi, E., Correll, D. L., Hauer, R., Pinay, G., Planty-Tabacchi, A. M., and Wissmar, R. C.: Development, maintenance and role of riparian vegetation in the river landscape, Freshwater Biol., 40, 497–516, 1998.

Thorp, J. H., Thoms, M. C., and Delong, M. D.: The riverine ecosystem synthesis: biocomplexity in river networks across space and time, River. Res. Appl., 22, 123–147, 2006.

US Army Corps of Engineers: Hydrologic Modeling System HEC-HMS, Technical Reference Manual, Hydrologic Engineering Center, Davis, CA, USA, 155 pp., 2000.

US Army Corps of Engineers: HEC-RAS river analysis system, Hydraulic Reference Manual ver. 3.1.3, 262 pp., Hydrologic Engineering Center, Davis, CA, USA, 2005.

US Department of Agriculture Forest Service (USDA FS): Watershed Protection and Management, Forest Service Manual Chapter 2520, 26, 1994.

US Department of Agriculture Natural Resource Conservation Service (USDA NRCS): General Manual, 190-GM, part 411, US Department of Agriculture Natural Resource Conservation Service (USDA NRCS), Washington DC, USA, 1991.

Van Coller, A. L., Rogers, K. H., and Heritage, G. L.: Riparian vegetation - environment relationships: complimentarity of gradients versus patch hierarchy approaches, J. Veg. Sci., 11, 337–350, 2000.

Verry, E. S., Dolloff, C. A., and Manning, M. E.: Riparian ecotone: a functional definition and delineation for resource assessment, Water Air Soil Poll., 4, 67–94, 2004.

Wolman, M. G. and Leopold, L. B.: River flood plains: some observations on their formation, US Geol. Surv. Prof. Pap, 282-C, 86–109, 1957.

Yang, Q., Mc Vicar, T., Van Niel, T., Hutchinson, M., Li, L., and Zhang, X.: Improving a digital elevation model by reducing source data errors and optimising interpolation algorithm parameters: an example in the Loess Plateau, China, Int. J. Appl. Earth Obs., 9, 235–246, 2007.

FIGURE CAPTATIONS

Figure 1. River network of the Cantabrian region, northern Spain, and spatial distribution of the three considered valley types over the study area.

Figure 2. Flowchart illustrating the methods used to delineate the hydrological and geomorphological floodplain surfaces and the GIS processes used to obtain coinciding and exceeding areas.

Figure 3. Floodplain cross-section defining the geomorphological parameters in which the BFD approach relies on.

Figure 4. Illustration of river centre-lines over the digital elevation model at a confluence (A) and bankfull depth floodplain surfaces (B; at 1, 2 and 3 bankfull depth heights) and path distance floodplain surfaces (C; at 100, 200 and 300 threshold values) at the same location.

Figure 5. Delineation of coinciding area (CA), 50-year flood exceeding area (T50EA) and geomorphological surface exceeding area (GSEA) to evaluate the adjustment between geomorphological (BFD-2) and hydrological criteria (50-yr flood) derived surfaces.

Figure 6. Boxplots of the four variables involved in the river reach classification for the three geomorphological valley types.

Figure 7. Adjustment parameters when using a 10-m DEM: coinciding area (CA), 50-year flood exceeding area (T50EA) and geomorphological surface exceeding area (GSEA) for bankfull depth (1, 3 and 5) and path distance (2, 4 and 6) approaches in open valleys (A), shallow vee valleys (B) and deep vee valleys (C).

Figure 8. Adjustment parameters when using a 30-m DEM: coinciding area (CA), 50-year flood exceeding area (T50EA) and geomorphological surface exceeding area (GSEA) for bankfull depth (1, 3 and 5) and path distance (2, 4 and 6) approaches in open valleys (A), shallow vee valleys (B) and deep vee valleys (C).

Figure 9. Values obtained for the two different methods used to evaluate the adjustment between geomorphological surfaces and the 50-year flood when using a

10-m DEM. Arrows indicate optimal threshold values (best adjustment) for each geomorphological approach and valley type.

Figure 10. Adjustment between the 50-yr flood and the optimal geomorphological floodplain surfaces in unconstrained (A and B) and constrained (C and D) valleys when using the BFD (A and C) and the PD (B and D) approaches.

Figure 11. Illustration of the floodprone area at 1.25-BFD over the digital elevation model: at a river confluence deriving in wider floodprone areas (A), at a river confluence not deriving in wider floodprone areas (B) and at an unconstrained-constrained-unconstrained valley transition (C).

FIG 1

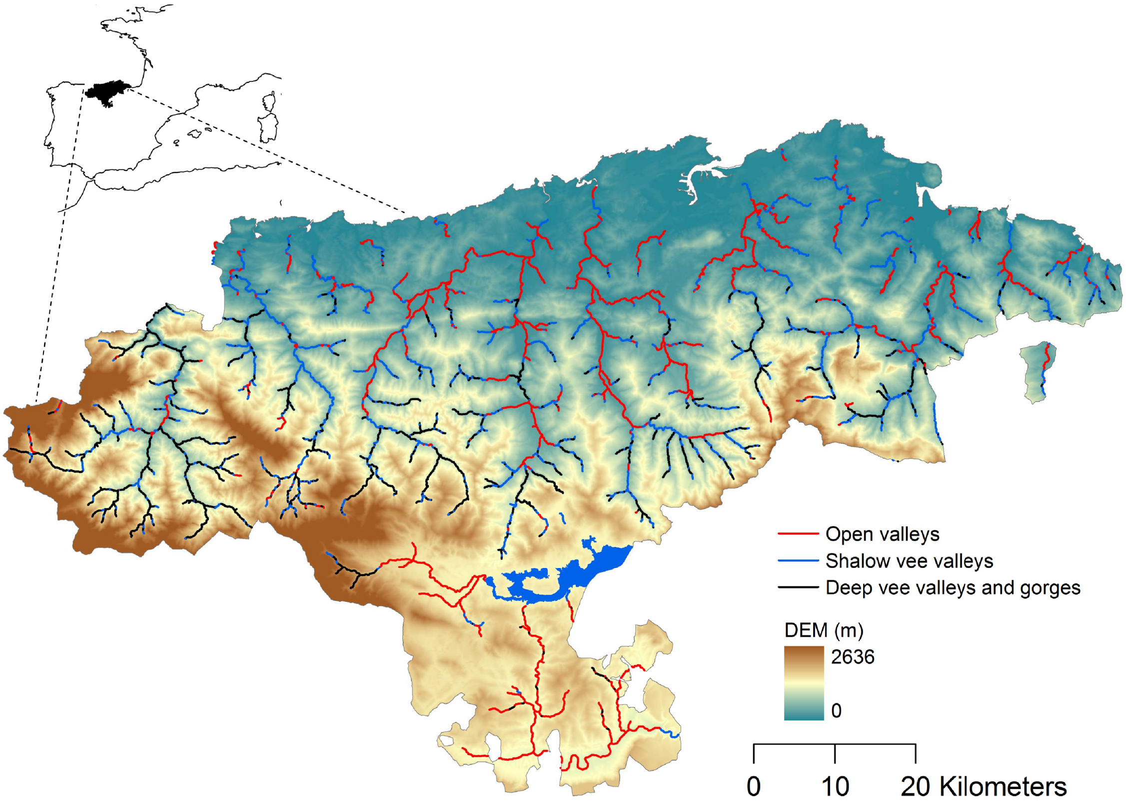
Open valleys
Shalow vee valleys
Deep vee valleys and gorges
DEM (m)
2636
0
0
10
20 Kilometers

1FIG 2

2

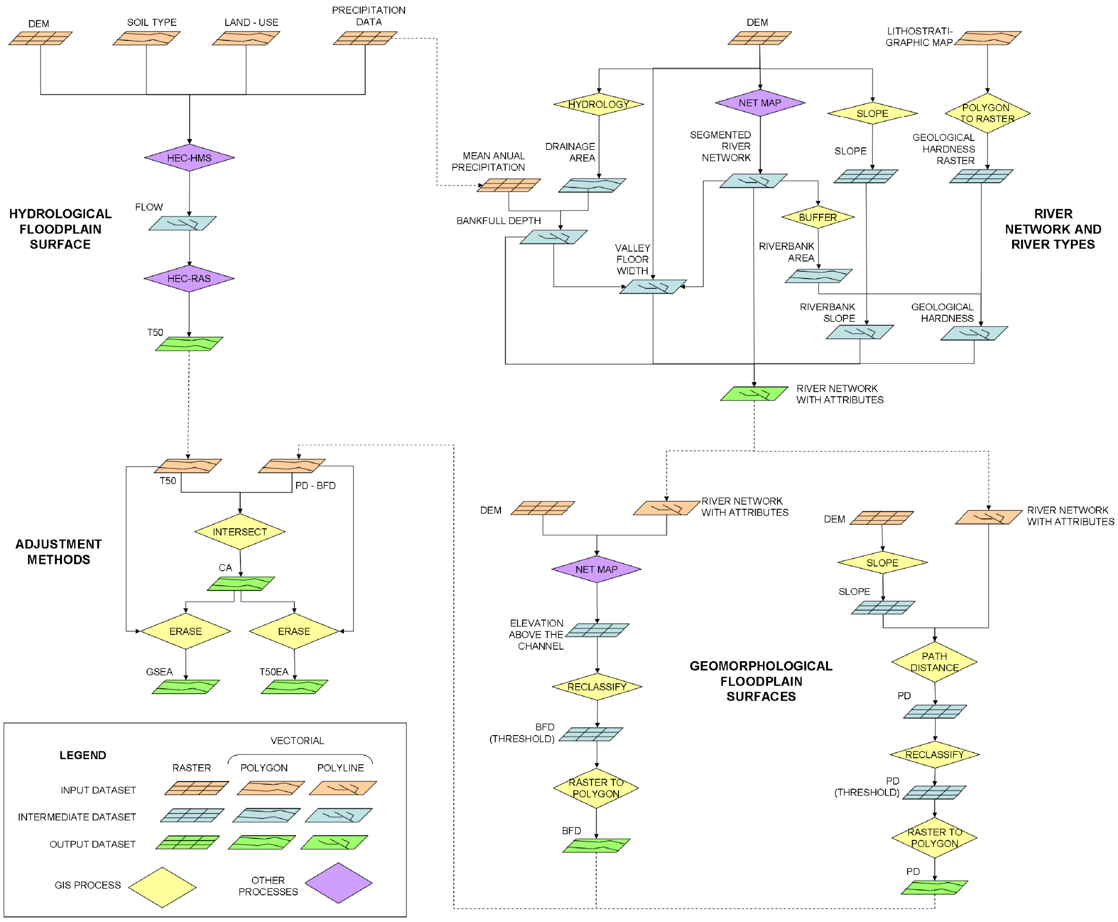
DEM
SOIL TYPE
LAND - USE
PRECIPITATION DATA
HEC-HMS
FLOW
HYDROLOGICAL FLOODPLAIN SURFACE
HEC-RAS
T50
DEM
LITHOSTRATI-GRAPHIC MAP
HYDROLOGY
NET MAP
SLOPE
POLYGON TO RASTER
MEAN ANUAL PRECIPITATION
DRAINAGE AREA
SEGMENTED RIVER NETWORK
SLOPE
GEOLOGICAL HARDNESS RASTER
BANKFULL DEPTH
BUFFER
RIVER NETWORK AND RIVER TYPES
VALLEY FLOOR WIDTH
RIVERBANK AREA
RIVERBANK SLOPE
GEOLOGICAL HARDNESS
RIVER NETWORK WITH ATTRIBUTES
T50
PD - BFD
ADJUSTMENT METHODS
INTERSECT
CA
ERASE
ERASE
GSEA
T50EA
DEM
RIVER NETWORK WITH ATTRIBUTES
DEM
RIVER NETWORK WITH ATTRIBUTES
NET MAP
SLOPE
SLOPE
ELEVATION ABOVE THE CHANNEL
GEOMORPHOLOGICAL FLOODPLAIN SURFACES
PATH DISTANCE
RECLASSIFY
PD
BFD (THRESHOLD)
RECLASSIFY
RASTER TO POLYGON
PD (THRESHOLD)
BFD
RASTER TO POLYGON
PD
LEGEND
VECTORIAL
RASTER
POLYGON
POLYLINE
INPUT DATASET
INTERMEDIATE DATASET
OUTPUT DATASET
GIS PROCESS
OTHER PROCESSES

3

FIG 3

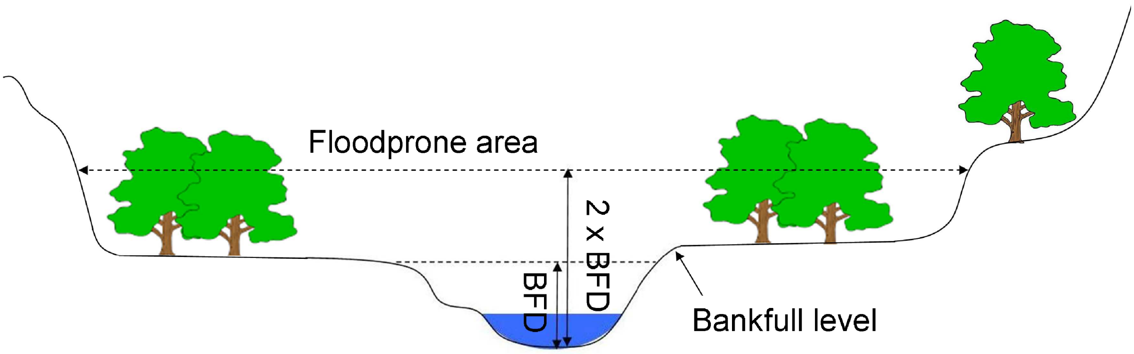

1FIG 4

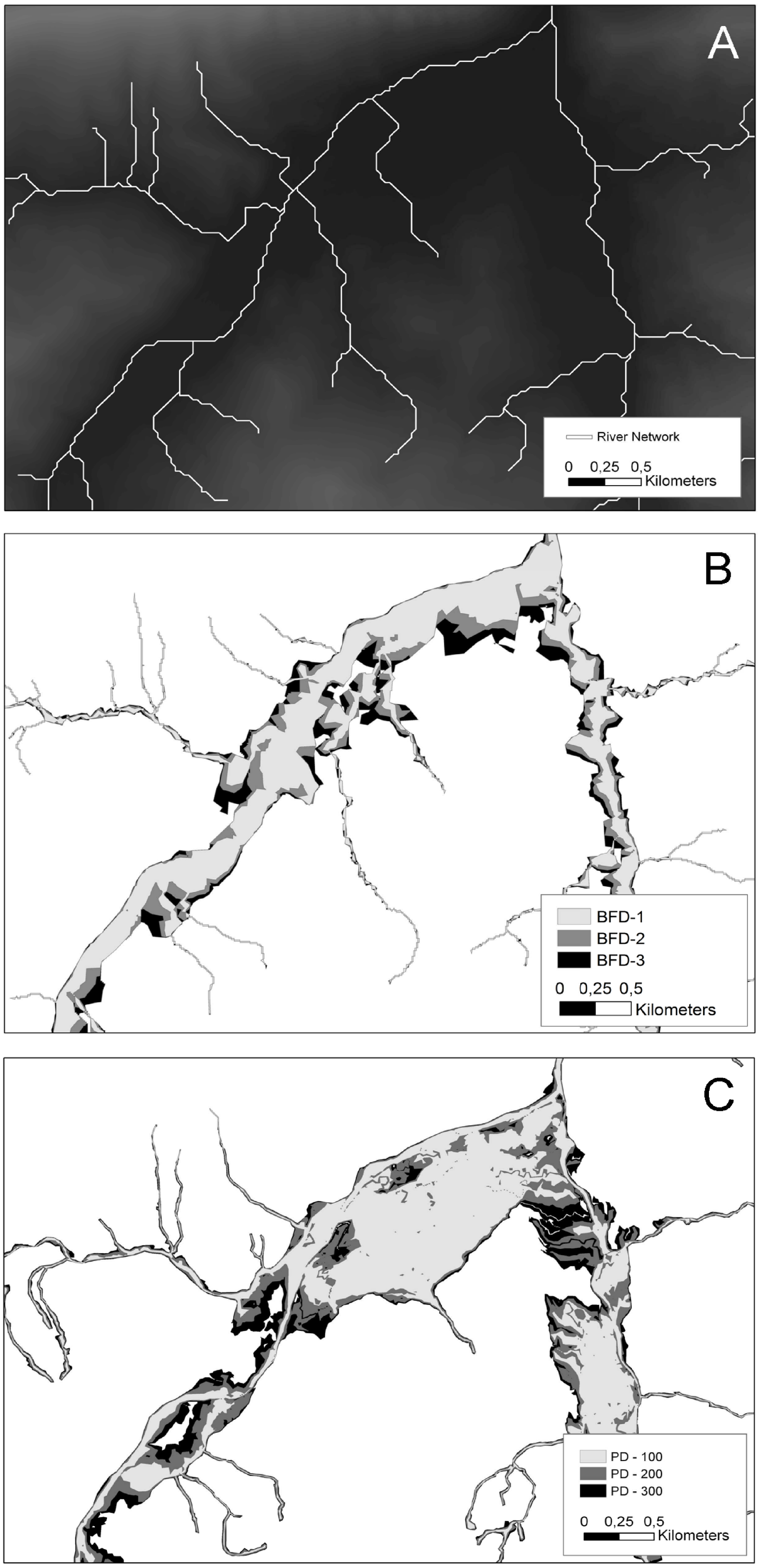
A
River Network
0 0,25 0,5
Kilometers
B
BFD-1
BFD-2
BFD-3
0 0,25 0,5
Kilometers
C
PD - 100
PD - 200
PD - 300
0 0,25 0,5
Kilometers

2

FIG 5


GEOMORPHOLOGICAL SURFACE (2*BFD)
0 0,25 0,5 Kilometers
50-YEAR FLOOD
0 0,25 0,5 Kilometers
CA
T50EA
GSEA
0 0,25 0,5 Kilometers

1FIG 6

2

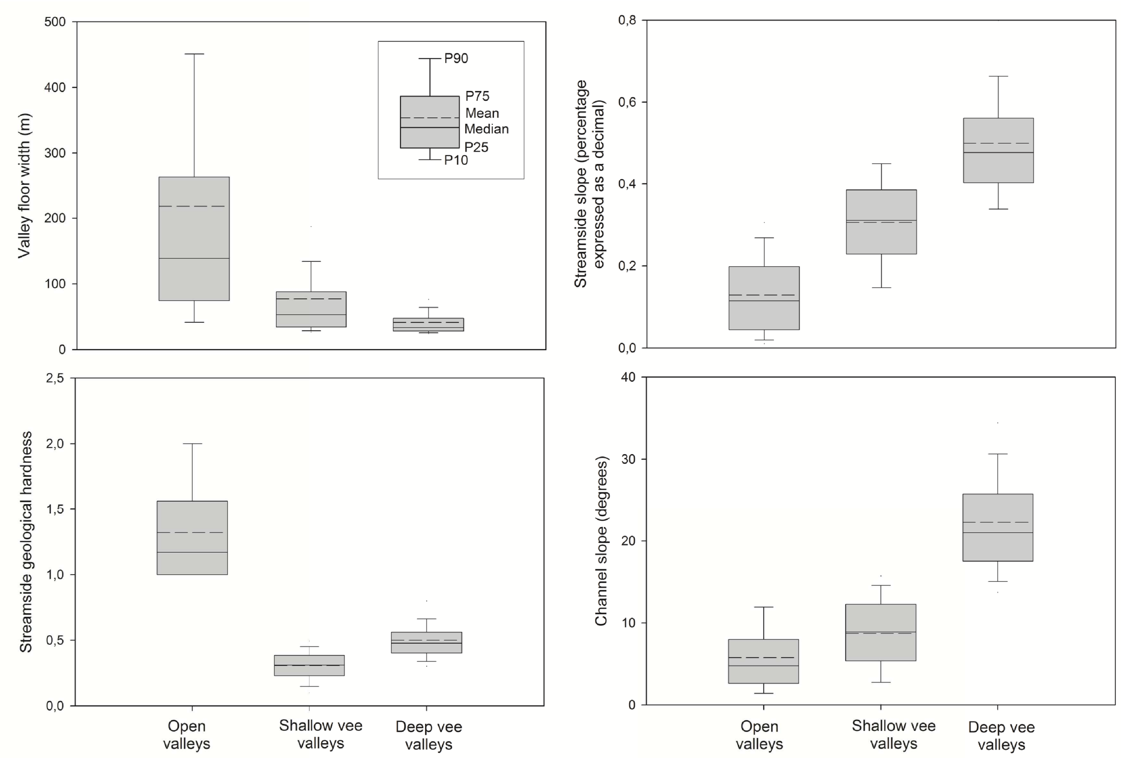
Valley floor width (m)
P90
P75
Mean
Median
P25
P10
Streamside slope (percentage expressed as a decimal)
Streamside geological hardness
Channel slope (degrees)
Open valleys
Shallow vee valleys
Deep vee valleys

3

1 FIG 7

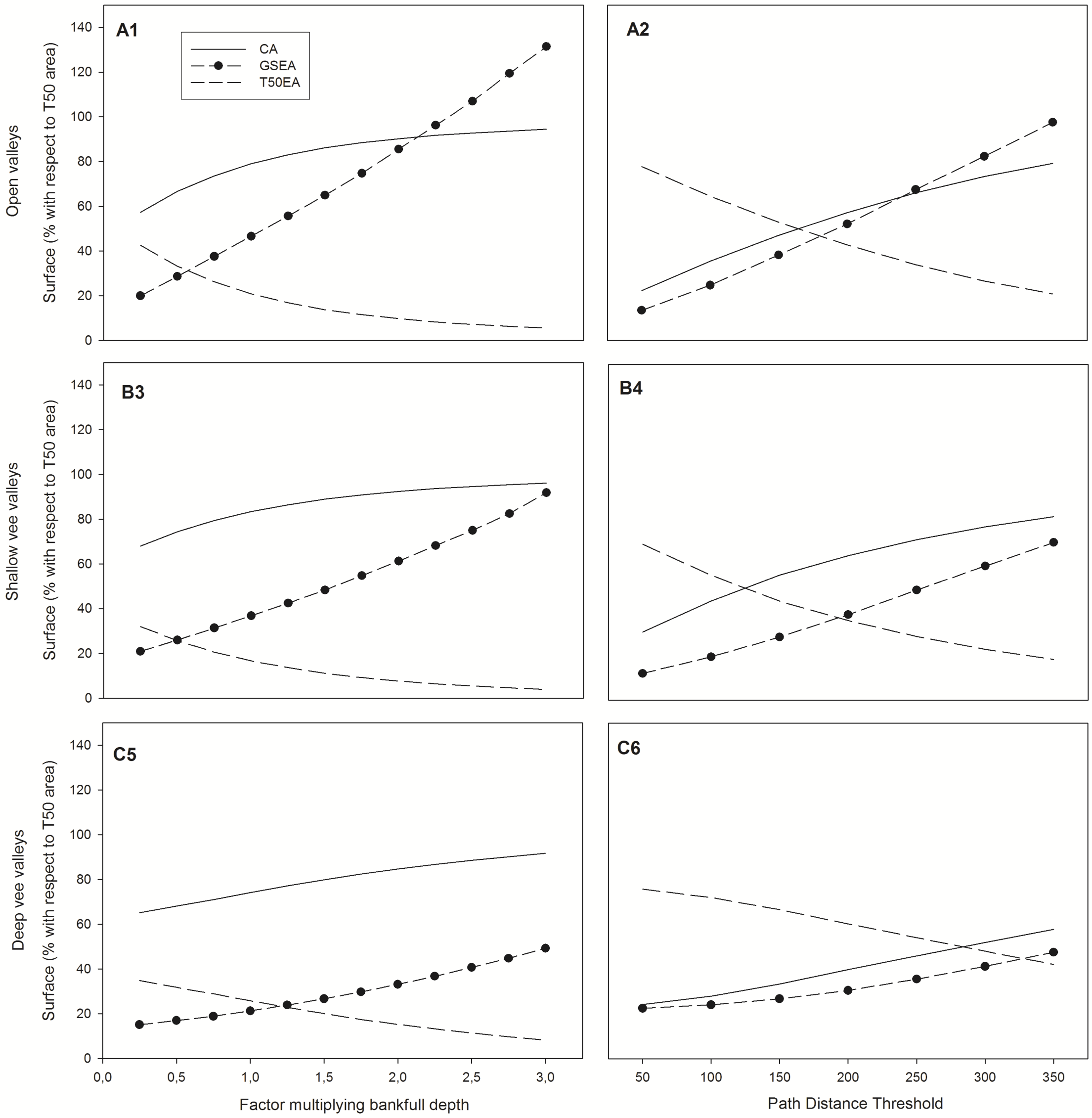
A1
A2
B3
B4
C5
C6
CA
GSEA
T50EA
Open valleys
Shallow vee valleys
Deep vee valleys
Surface (% with respect to T50 area)
Factor multiplying bankfull depth
Path Distance Threshold
0
20
40
60
80
100
120
140
0,0
0,5
1,0
1,5
2,0
2,5
3,0
50
100
150
200
250
300
350

2

1FIG 8

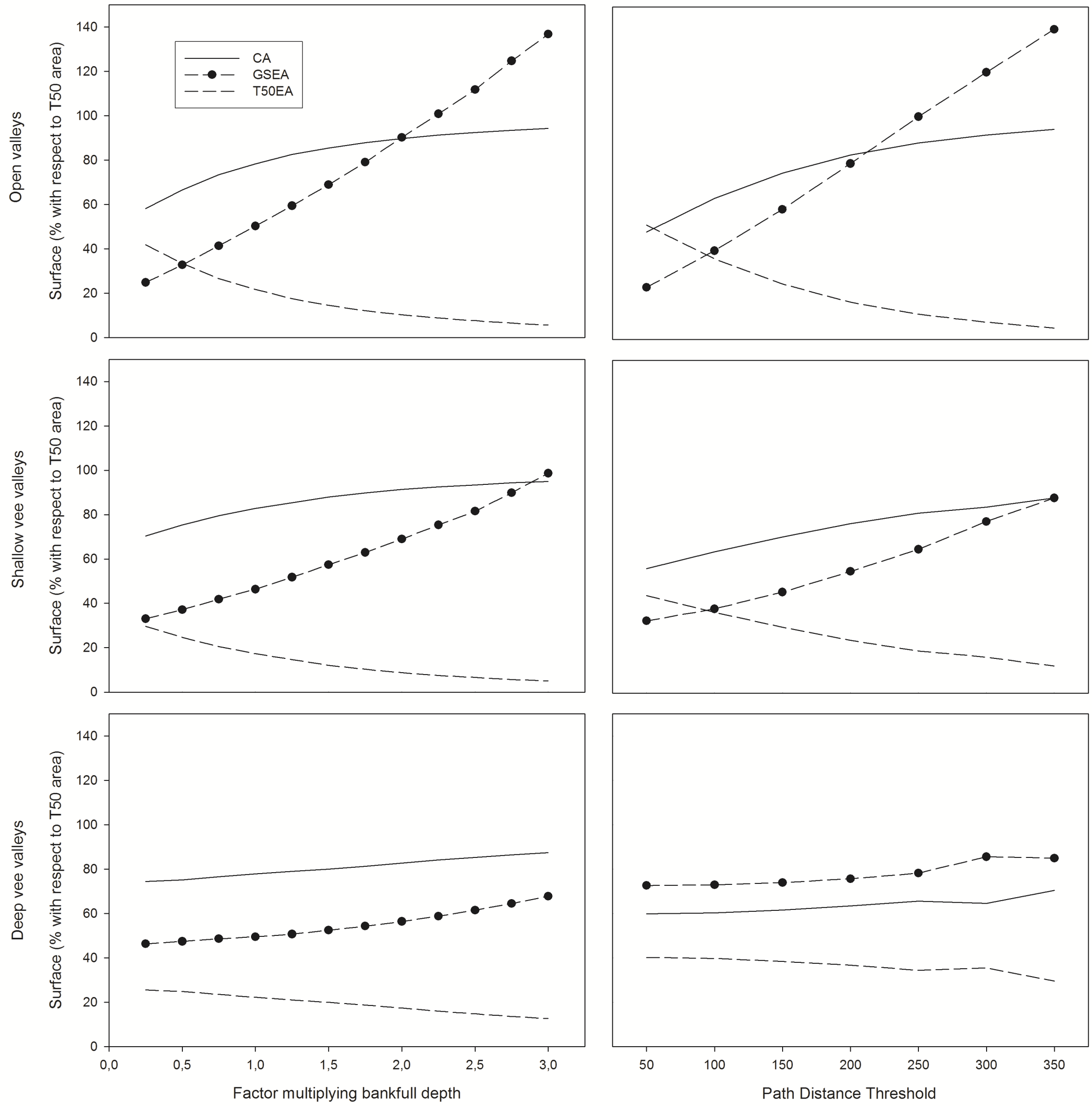

CA
GSEA
T50EA
Open valleys
Shallow vee valleys
Deep vee valleys
Surface (% with respect to T50 area)
0
20
40
60
80
100
120
140
0,0
0,5
1,0
1,5
2,0
2,5
3,0
Factor multiplying bankfull depth
50
100
150
200
250
300
350
Path Distance Threshold

2

FIG 9

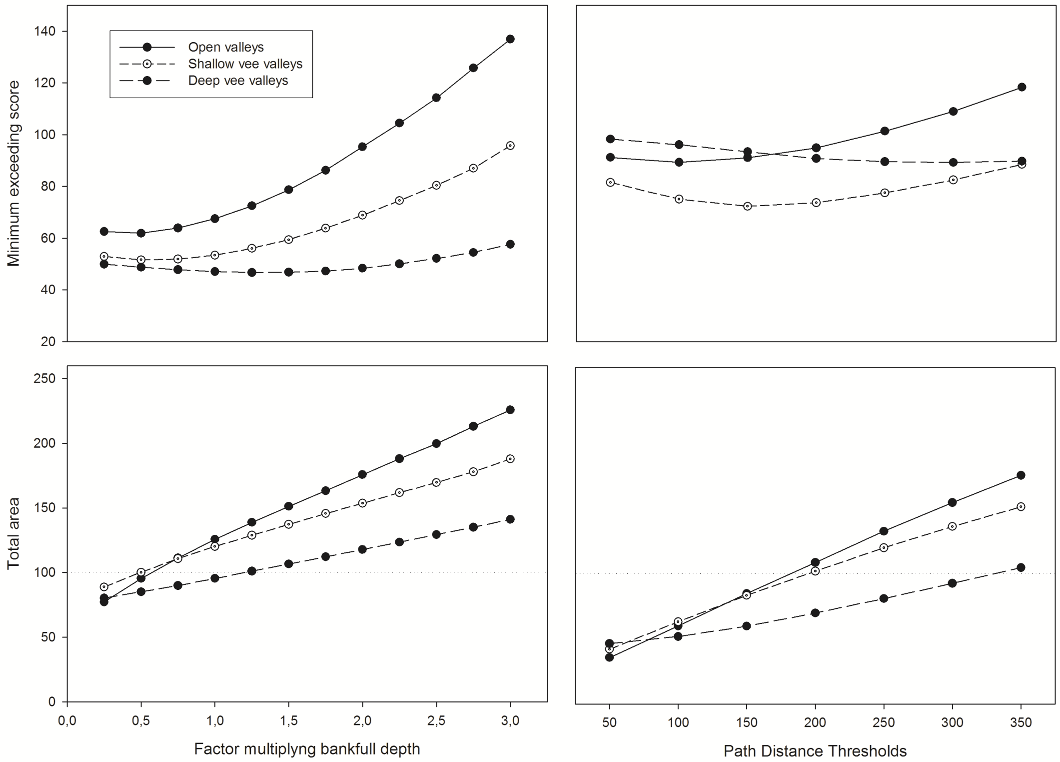

Open valleys
Shallow vee valleys
Deep vee valleys
Minimum exceeding score
Total area
Factor multiplyng bankfull depth
Path Distance Thresholds

FIG 10

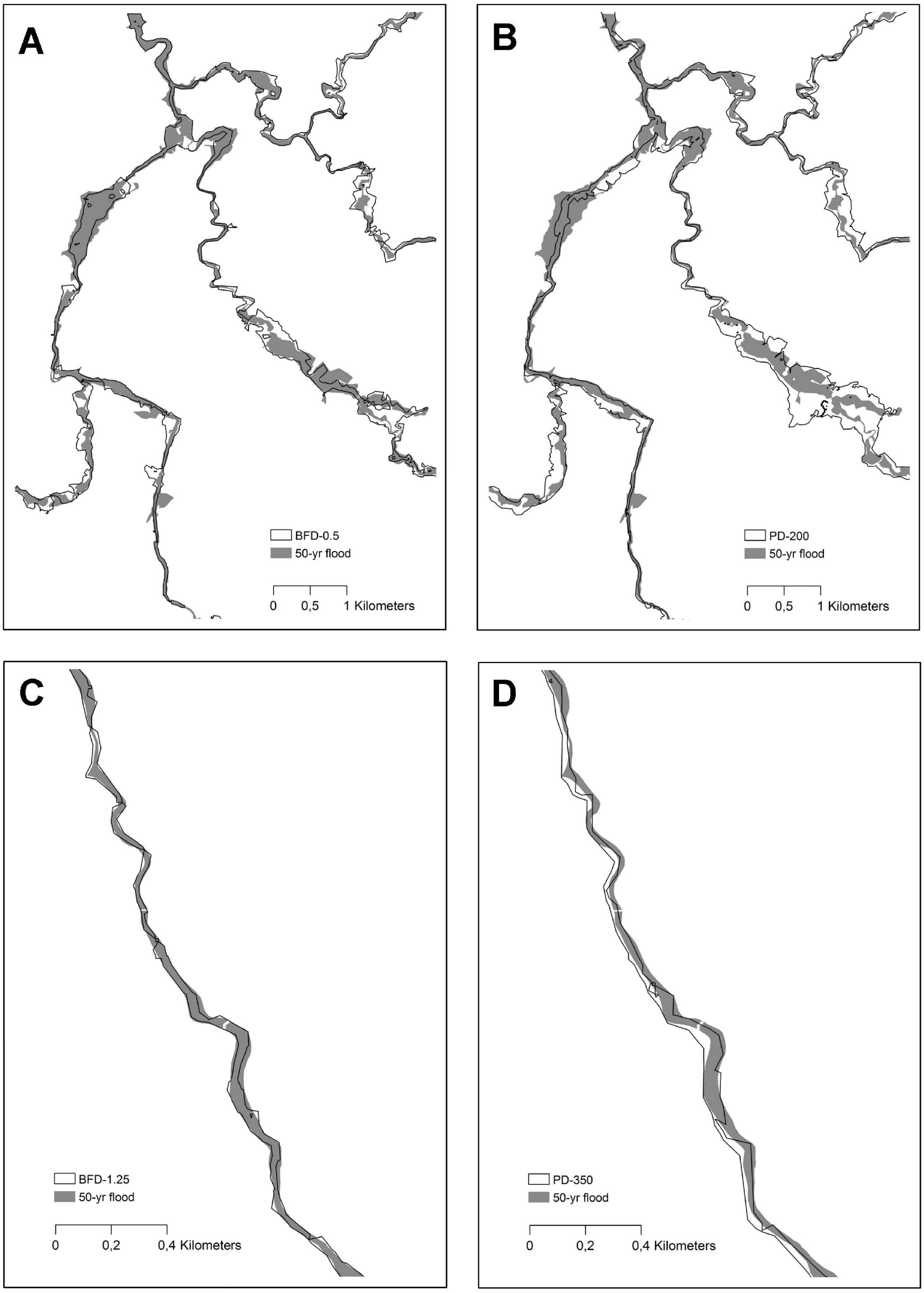
A
BFD-0.5
50-yr flood
0 0,5 1 Kilometers
B
PD-200
50-yr flood
0 0,5 1 Kilometers
C
BFD-1.25
50-yr flood
0 0,2 0,4 Kilometers
D
PD-350
50-yr flood
0 0,2 0,4 Kilometers

FIG 11

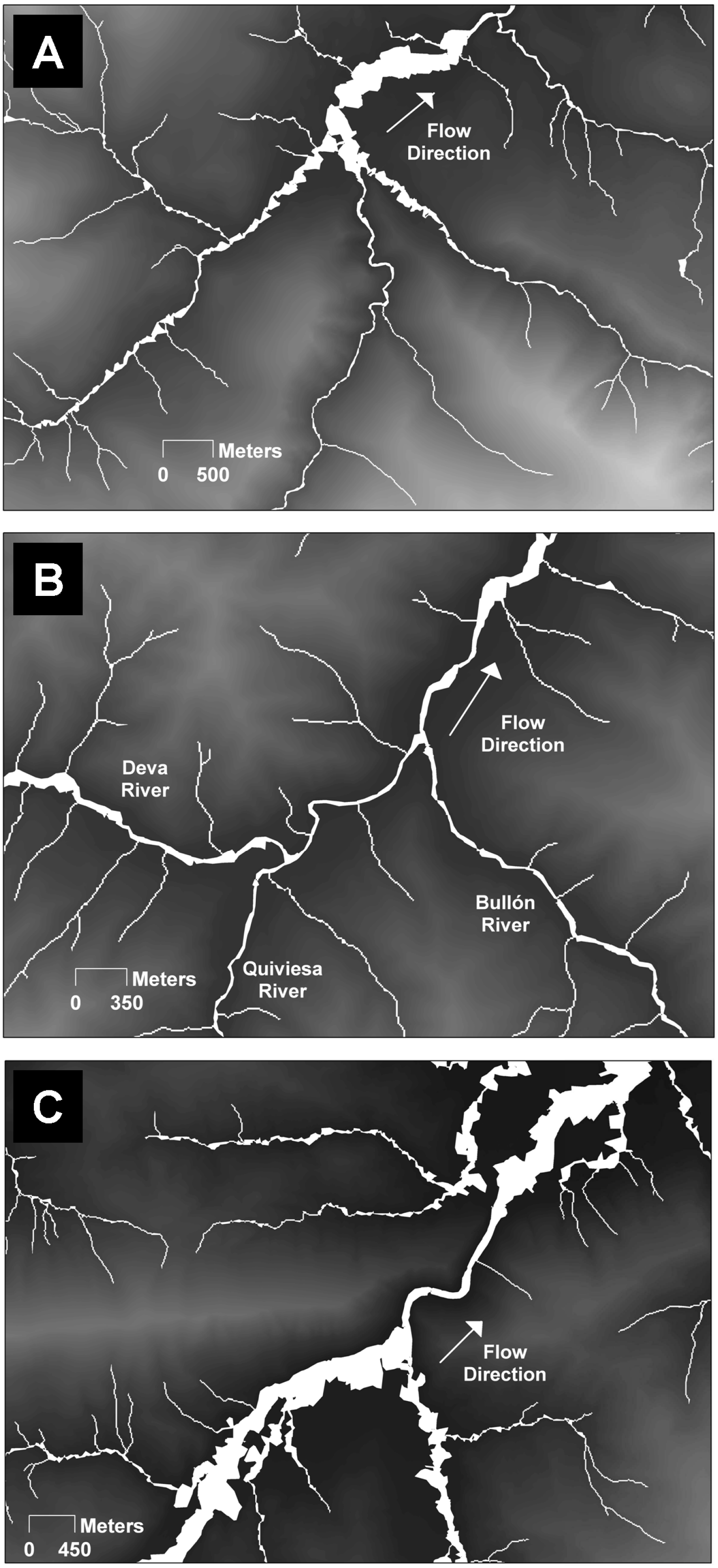
A
Flow
Direction
Meters
0 500
B
Flow
Direction
Deva
River
Bullón
River
Quiviesa
River
Meters
0 350
C
Flow
Direction
Meters
0 450